Journal of The Electrochemical Society, **149** (7) B340-B347 (2002)
0013-4651/2002/149(7)/B340/8/$7.00 © The Electrochemical Society, Inc.

Electrochemistry of Copper in Aqueous Ethylenediamine Solutions

Serdar Aksu and Fiona M. Doyle[*,z]

Department of Materials Science and Engineering, University of California at Berkeley, Berkeley, California 94720-1760, USA

Potential-pH equilibria and potentiodynamic polarization studies were used to examine the electrochemical behavior of copper in aqueous ethylenediamine solutions. Potential-pH diagrams for the copper-water-ethylenediamine system were derived at different total copper $\{Cu_T\}$ and ethylenediamine $\{En_T\}$ activities. The diagrams show that the solubility range of copper is significantly extended in the presence of ethylenediamine. Polarization experiments were conducted in deaerated and aerated aqueous solutions of 10^{-2} M ethylenediamine with 10^{-3} M cupric sulfate, and 10^{-4} M ethylenediamine with 10^{-5} M cupric sulfate over a wide pH range. The results of these experiments are discussed in terms of relevant potential-pH diagrams. Good correlations were observed.

Manuscript submitted August 22, 2001; revised manuscript received January 23, 2002. Available electronically May 16, 2002.

The electrochemical behavior of copper in complexing agents is of great importance in various fields of electrochemistry, especially in corrosion and electrodeposition studies. Being a relatively noble metal, copper is immune to corrosion in noncomplexing solutions that are free from oxidizing agents. It becomes susceptible to corrosive attack only in highly acidic or alkaline solutions containing oxidizing agents, as indicated by the potential-pH diagrams of the Cu-H_2O system.[1] Complexing agents such as ammonia, cyanide, and glycine significantly lower the corrosion resistance of copper in aqueous solutions. Potential-pH diagrams for the Cu-CN^--H_2O,[2] Cu-NH_3-H_2O,[3] and Cu-glycine-H_2O[4] systems show a considerable expansion in the solubility domain of copper due to the complexation of Cu^{2+} and Cu^+ ions.

Ethylenediamine is an organic complexing agent that finds several applications in industrial electrochemical processes involving copper. Since ethylenediamine can chelate and effectively stabilize both cupric and the cuprous ions in aqueous solutions, it is used as a bath additive for noncyanide alkaline electroplating of copper.[5-8] It is also widely utilized in oxidative dissolution of copper metal or oxides for removal from the sludges deposited in the secondary side of the steam generator of nuclear power plants.[9,10] Metal complexes of ethylenediamine are being investigated as potential reducing agents in electroless copper deposition.[11]

Halpern and co-workers[12] investigated the kinetics of the dissolution of copper in aqueous ethylenediamine solutions. The dissolution behavior in ethylenediamine was similar to that with complexing agents such as ammonia,[13] glycine, α-alanine, and β-alanine.[14] In each case, the rate was zero order in oxygen and first order in the complexing agent above a critical partial pressure of oxygen. Below the critical oxygen partial pressures, the rate of copper dissolution was proportional to the oxygen partial pressure, and independent of the concentration of complexing agent. For both ammonia and ethylenediamine, the dissolution rate was lower at more alkaline pH values, indicating that the protonated complexing species were more reactive than the neutral, base complexing species. Jenkins[15] observed that the rate of dissolution of single crystalline copper was independent of the crystallographic orientation of the exposed metal surface in aqueous ethylenediamine solutions containing oxygen.

El-Sayed and collaborators studied the corrosion of copper in aqueous ethylenediamine solutions and in solutions of some transition metal-ethylenediamine complexes. The corrosion rate of copper decreased in the following order: En ≫ Cu complex ≫ Cd complex > Zn complex > Ni complex.[16] Survila *et al.*[17,18] recently analyzed thermodynamic and kinetic aspects of Cu_2O formation in ethylenediamine. Their work indicates that copper solubility expands over a wider pH range in the presence of ethylenediamine. They found that two separate regions of Cu_2O stability can exist in slightly acidic and strongly alkaline media.

The current study aims to increase our fundamental understanding of the electrochemical behavior of copper in ethylenediamine solutions. First, the thermodynamics of copper complexation in aqueous ethylenediamine solutions are analyzed to produce potential-pH diagrams for the copper-ethylenediamine-water system. Experimental measurements of polarization behavior of copper in ethylenediamine solutions of different compositions are then reported and discussed in terms of the relevant potential-pH diagrams.

Potential-pH Diagrams for the Copper-Ethylenediamine-Water System

Ethylenediamine can exist in aqueous solutions in three different forms: $^+H_3N\text{-}CH_2\text{-}CH_2\text{-}NH_3^+$, $^+H_3N\text{-}CH_2\text{-}CH_2\text{-}NH_2$, and $H_2N\text{-}CH_2\text{-}CH_2\text{-}NH_2$. These species are denoted as H_2En^{2+}, HEn^+, and En, respectively. The equilibria between these may be depicted as[19]

$$\underset{(H_2En^{2+})}{^+H_3N\text{-}CH_2\text{-}CH_2\text{-}NH_3^+} \overset{pK_{a1}=6.848}{\leftrightarrow} \underset{(HEn^+)}{^+H_3N\text{-}CH_2\text{-}CH_2\text{-}NH_2} \overset{pK_{a2}=9.928}{\leftrightarrow} \underset{(En)}{H_2N\text{-}CH_2\text{-}CH_2\text{-}NH_2} \quad [1]$$

As shown in Fig. 1, H_2En^{2+} predominates at pH values below 6.848 (pK_{a1}), while En predominates at pH values above 9.928 (pK_{a2}). HEn^+ predominates at intermediate pH values. Ethylenediamine forms soluble complexes with both cupric and cuprous ions. The principal copper(II) ethylenediamine complexes are $Cu(H_2N\text{-}CH_2\text{-}CH_2\text{-}NH_2)^{2+}$, $Cu(H_2N\text{-}CH_2\text{-}CH_2\text{-}NH_2)_2^{2+}$, $Cu(H_2N\text{-}CH_2\text{-}CH_2\text{-}NH_2)_3^{2+}$, and $CuOH(H_2N\text{-}CH_2\text{-}CH_2\text{-}NH_2)_2^+$, while the principal Cu(I) species is $Cu(H_2N\text{-}CH_2\text{-}CH_2\text{-}NH_2)_2^+$. These are referred to as $CuEn^{2+}$, $CuEn_2^{2+}$, $CuEn_3^{2+}$, $CuOHEn_2^+$, and $CuEn_2^+$, respectively.

The principles involved in calculating and plotting potential-pH diagrams were recently reviewed.[4] Table I presents the association constants of the copper-ethylenediamine complexes identified above.[19,20] These were used to calculate the stabilities of the individual species. Table II lists the standard Gibbs free energies of formation of species in the copper-water system.[21] Cupric hydroxide, $Cu(OH)_2$, was not considered because it is less stable than cupric oxide.[1] Table III shows all thermodynamically meaningful reactions between the species in the copper-water-ethylenediamine system, along with the equations of each equilibrium line, calculated using the data provided in Tables I and II, following the procedure previously reported.[4]

* Electrochemical Society Active Member.
[z] E-mail: fiona@socrates.berkeley.edu

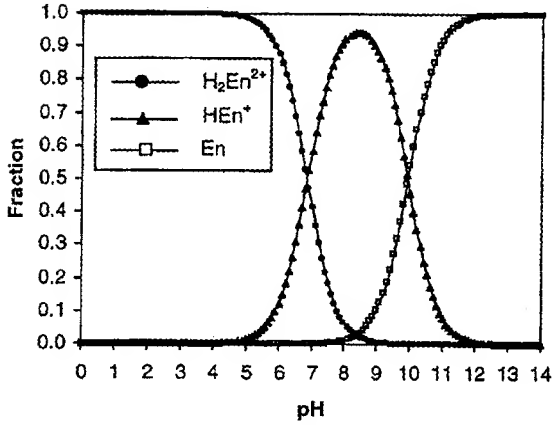

Figure 1. Distribution of ethylenediamine species as a function of pH in the ethylenediamine-water system at 25°C.

Figure 2 shows potential-pH diagrams plotted from the equilibria in Table III at various combinations of total ethylenediamine activity, $\{En_T\}$, and total dissolved Cu activity, $\{Cu_T\}$. The lines identified as 1 to 4 correspond to the equations of the same number in Table III. Figure 2 demonstrates that copper metal is oxidized to form copper(II) ethylenediamine species, either $CuEn^{2+}$ or $CuEn_2^{2+}$, over a wide range of pH values. At high $\{En_T\}$ to $\{Cu_T\}$ ratios (Fig. 2c and d), the $CuOHEn_2^+$ complex becomes dominant at alkaline pH values. The copper(I) ethylenediamine complex, $CuEn_2^+$, only appears when $\{En_T\}$ is much higher than $\{Cu_T\}$ (Fig. 2c), such that the line for reduction of $CuEn_2^+$ to elemental copper is below the line for reduction of $CuEn_2^{2+}$ to $CuEn_2^+$. Although the activity of the $CuEn_3^{2+}$ complex increases as $\{En_T\}$ increases, this species becomes dominant only at exceedingly high $\{En_T\}$ (above about 8). Therefore, it does not appear for the combinations of $\{En_T\}$ and $\{Cu_T\}$ considered in Fig. 2. Note that ethylenediamine is in the neutral form (En) when complexing copper, even at acidic pH values. $CuEn_2^{2+}$ has a much wider stability region than $CuEn^{2+}$, which is expected due to the higher entropy change associated with the formation of the former complex. For the combinations of $\{En_T\}$ and $\{Cu_T\}$ considered in Fig. 2, the only anionic hydrolyzed Cu(II) species to appear at high pH values is CuO_2^{2-}; $HCuO_2^-$ never predominates. The stability regions of cupric oxide, CuO, and cuprous oxide, Cu_2O, expand with increasing $\{Cu_T\}$ and contract with increasing $\{En_T\}$. Figures 2a and b show two separate regions of Cu_2O stability, under slightly acid and strongly alkaline conditions, consistent with previous studies.[17,18]

We emphasize that potential-pH diagrams only provide information about thermodynamic equilibrium and infer nothing about the kinetics of reactions. Moreover, although underlying metals may be passive in regions where oxides predominate, they need not be; passivation requires coherent, adherent oxide films with low conductivity. Nevertheless, potential-pH diagrams have proved useful in elucidating the electrochemistry of copper in various aqueous media.[2-4,22-24]

Table I. Association constants of En and copper-En species at 25°C and 1 atm (I is the ionic strength at which the data were acquired, from Ref. 20 and 21).

Reaction	Logarithm of the stability constant at 25°C and 1 atm	
$En_2 + H^+ = HEn^+$	9.928	($I = 0$)
$HEn^+ + H^+ = H_2En^{2+}$	6.848	($I = 0$)
$Cu^{2+} + En = CuEn^{2+}$	10.50	($I = 0$)
$Cu^{2+} + 2En = CuEn_2{}^{2+}$	19.6	($I = 0$)
$CuEn_2^{2+} + En = CuEn_3^{2+}$	−0.9	($I = 1$)
$CuEn^{2+} + OH^- = CuOHEn_2^+$	0.73	($I = 0.5$)
$Cu^+ + 2En = CuEn_2^+$	11.2	($I = 0.3$)

Table II. Standard Gibbs free energies of formation of species in the copper-water system at 25°C and 1 atm (from Ref. 22).

Species	State	ΔG_f^0 (kJ/mol)
H^+	Aqueous	0
OH^-	Aqueous	−117.244
H_2O	Liquid	−237.129
H_2	Gas	0
O_2	Gas	0
Cu^+	Aqueous	49.98
Cu^{2+}	Aqueous	65.49
Cu	Solid	0
CuO	Solid	−129.7
Cu_2O	Solid	−146.0
CuO_2^{2-}	Aqueous	−183.6
$HCuO_2^-$	Aqueous	−258.5

Experimental

Reagents and solutions.—Ethylenediamine (>99%) was obtained from Acros Organics Co. Reagent grade cupric sulfate was purchased from Fisher Scientific Co. Electrolyte solutions were prepared using double distilled water, and their pH was adjusted to ±0.1 units using NaOH or H_2SO_4 (both reagent grade from Fisher Scientific Co.). The solutions at pH 4.5 and 5.5 were buffered using acetic acid/sodium acetate. No additional buffering agents were needed at higher pH values because of the buffering action of HEn^+/En. The electrolyte was either aerated or deaerated before use. For aeration, breathing (medical) air was purged into the electrolyte through a porous gas disperser for 18 h. After aeration, the pH was adjusted with NaOH to correct for absorption of CO_2. For deaeration, ultrapure nitrogen gas (99.999 % N_2) was sparged for 24 h; this did not affect the pH.

Electrochemical cell.—Polarization studies were made using three-electrode cells. Each cylindrical glass cell was 130 mm high, with a 120 mm interior diam. The Plexiglas cell lid had openings for a glass Luggin probe, gas disperser, and working and counter electrodes. When purging air or nitrogen into the solution, the cell was sealed except for openings on the lid less than 2 mm diam, which allowed the discharge of excess gas. The working electrode was a copper disk constructed from a 10 mm diam rod of 99.9999% pure copper (Aldrich Chemical Co.), embedded in a nonconductive, nonreactive epoxy (Tra-Con Inc.). The outer diam of the electrode was 25.4 mm. The electrode was first ground to a 600 grit finish, then rinsed in water and acetone, and dried. It was then mirror-polished with a succession of diamond pastes from 9 to 0.25 μm and finally cleaned with acetone and distilled water. The electrode was rotated at 200 rpm using a Pine Instrument Co. electrode rotator. A reference saturated calomel electrode (SCE) [0.242 V standard hydrogen electrode (SHE)] was held in a Luggin probe filled with the same solution as the electrochemical cell. The tip of the probe was held about 2 mm from the working electrode. A platinum mesh counter electrode was held 20 mm from, and parallel to, the working electrode. All potentials are reported with respect to the SHE. They are uncorrected for liquid junction potentials (E_{LJP}) and ohmic potential drops (E_{IR}). The liquid junction potential between the SCE containing about 4.66 M saturated KCl and the ethylenediamine test solutions with copper sulfate was estimated using the Henderson equation[25] and the equivalent conductance of the potassium, chloride, cupric, and sulfate ions.[26] Assuming that ethylenediamine has

Table III. Equilibria in the copper-water-ethylenediamine system at 25°C and 1 atm.

Number	Reaction	Equilibrium line
1	$O_2 + 4H^+ + 4e = 2H_2O$	$E = 1.229 - 0.059pH$
2	$2H^+ + 2e = H_2$	$E = -0.059pH$
3	$HEn^+ + H^+ = H_2En^{2+}$	$pH = 6.848 + \log\{HEn^+\}/\{H_2En^{2+}\}$
4	$En + H^+ + HEn^+$	$pH = 9.928 + \log\{En\}/\{HEn^+\}$
5	$Cu^{2+} + 2e = Cu$	$E = 0.339 + 0.030 \log\{Cu^{2+}\}$
6	$Cu_2O + 2H^+ + 2e = 2Cu + H_2O$	$E = 0.472 - 0.059pH$
7	$2CuO + 2H^+ + 2e = Cu_2O + H_2O$	$E = 0.641 - 0.059pH$
8	$CuO + H_2O = CuO_2^{2-} + 2H^+$	$pH = 16.05 + 0.5 \log\{CuO_2^{2-}\}$
9	$CuO_2^{2-} + 4H^+ + 2e = Cu + 2H_2O$	$E = 1.506 - 0.118pH + 0.059 \log\{CuO_2^{2-}\}$
10	$2CuO_2^{2-} + 6H^+ + 2e^- = Cu_2O + 3H_2O$	$E = 2.540 - 0.1773pH + 0.059 \log\{CuO_2^{2-}\}$
11	$2Cu^{2+} + H_2O + 2e = Cu_2O + 2H^+$	$E = 0.207 + 0.059 \log\{Cu^{2+}\} + 0.059pH$
12	$Cu^{2+} + H_2En^{2+} = CuEn^{2+} + 2H^+$	$pH = 3.138 - 0.5 \log\{H_2En^{2+}\} + 0.5 \log\{CuEn^{2+}\}/\{Cu^{2+}\}$
13	$CuEn^{2+} + H_2En^{2+} = CuEn_2^{2+} + 2H^+$	$pH = 3.838 - 0.5 \log\{H_2En^{2+}\} + 0.5 \log\{CuEn_2^{2+}\}/\{CuEn^{2+}\}$
14	$CuEn^{2+} + 2H^+ + 2e^- = Cu + H_2En^{2+}$	$E = 0.525 - 0.059pH + 0.030 \log\{CuEn^{2+}\} - 0.030 \log\{H_2En^{2+}\}$
15	$CuEn_2^{2+} + 4H^+ + 2e^- = Cu + 2H_2En^{2+}$	$E = 0.752 - 0.118pH + 0.030 \log\{CuEn_2^{2+}\} - 0.059 \log\{H_2En^{2+}\}$
16	$CuEn_2^{2+} + 2H^+ + 2e^- = Cu + 2HEn^+$	$E = 0.347 - 0.059pH + 0.030 \log\{CuEn_2^{2+}\} - 0.059 \log\{HEn^+\}$
17	$CuEn_2^{2+} + 2e^- = Cu + 2En$	$E = -0.241 + 0.030 \log\{CuEn_2^{2+}\} - 0.059 \log\{En\}$
18	$CuO + 2H^+ + 2En = CuEn_2^{2+} = H_2O$	$pH = 13.48 + \log\{En\} - 0.5 \log\{CuEn_2^{2+}\}$
19	$2CuEn_2^{2+} + H_2O + 2e^- = Cu_2O + 2H^+ + 4En$	$E = -0.954 + 0.059pH + 0.059 \log\{CuEn_2^{2+}\} - 0.118 \log\{En\}$
20	$CuO_2^{2-} + 4H^+ + 2En = CuEn_2^{2+} + 2H_2O$	$pH = 14.76 + 0.5 \log\{En\} + 0.25 \log\{CuO_2^{2-}\}/\{CuEn_2^{2+}\}$
21	$CuEn_2^+ + 2H^+ + e^- = Cu + 2HEn^+$	$E = 1.030 - 0.118pH + 0.059 \log\{CuEn_2^{2+}\} - 0.118 \log\{HEn^+\}$
22	$CuEn_2^+ + e^- = Cu + 2En$	$E = -0.145 + 0.059 \log\{CuEn_2^+\} - 0.118 \log\{En\}$
23	$CuEn_2^{2+} + e^- = CuEn_2^+$	$E = -0.336 + 0.059 \log\{CuEn_2^{2+}\}/\{CuEn_2^+\}$
24	$Cu_2O + 2H^+ + 4En = 2CuEn_2^+ + H_2O$	$pH = 10.41 + 2 \log\{En\} - \log\{CuEn_2^+\}$
25	$2CuEn^{2+} + H_2O + 2H^+ + 2e^- = Cu_2O + 2H_2En^{2+}$	$E = 0.587 - 0.059pH + 0.059 \log\{CuEn^{2+}\} - 0.059 \log\{H_2En^{2+}\}$
26	$2CuEn_2^{2+} + H_2O + 6H^+ + 2e^- = Cu_2O + 4H_2En^{2+}$	$E = 1.054 - 0.177pH + 0.059 \log\{CuEn_2^{2+}\} - 0.118 \log\{H_2En^{2+}\}$
27	$CuEn_2^{2+} + H_2O = CuOHEn_2^+ + H^+$	$pH = 13.27 + \log\{CuOHEn_2^+\}/\{CuEn_2^{2+}\}$
28	$CuOHEn_2^+ + H^+ + e^- = Cu + 2En + H_2O$	$E = 0.152 - 0.030pH + 0.030 \log\{CuOHEn_2^+\} - 0.059 \log\{En\}$
29	$2CuOHEn_2^+ + 2e^- = Cu_2O + 4En + H_2O$	$E = -0.169 + 0.059 \log\{CuOHEn_2^+\} - 0.118 \log\{En\}$
30	$CuO_2^{2-} + 3H^+ + 2En = CuOHEn_2^+ + H_2O$	$pH = 15.261 + 0.667 \log\{En\} + \log\{CuO_2^{2-}\}/\{CuOHEn_2^+\}$
31	$CuOHEn_2^+ + H^+ + e^- = CuEn_2^+ + H_2O$	$E = 0.449 - 0.030pH + 0.059 \log\{CuOHEn_2^+\}/\{CuEn_2^+\}$

negligible contribution, the maximum E_{LJP}, about 5.7 mV, was in 10^{-4} M ethylenediamine solutions with 10^{-5} $CuSO_4$.

Polarization tests.—DC potentiodynamic polarization studies were made using a computer-controlled EG&G PAR model 273-A potentiostat. Tests were conducted in 650 mL of nitrogen- or air-purged aqueous solutions of either 10^{-2} M ethylenediamine with 10^{-3} M cupric sulfate or 10^{-4} M ethylenediamine with 10^{-5} M cupric sulfate at 24 ± 1°C. Air or nitrogen was purged during the experiments. Before each potentiodynamic scan, the copper electrode was allowed about 900 s to attain a stable open-circuit potential (E_{OC}). Potentiodynamic polarization curves were obtained by scanning at 1 mV/s, from 500 mV below E_{OC} to 1500 mV above.

Linear polarization resistance measurements were used to estimate the current densities (i_{OC}) at E_{OC}. In these experiments, the electrode was scanned at 0.2 mV/s from −40 mV below to 40 mV above E_{OC}. A plot of overpotential (η) from E_{OC} *vs.* current density (i) should be linear near E_{OC}, and the slope of such a plot gives the polarization resistance, R_p. The i_{OC} is inversely proportional to the R_p[27,28]

$$i_{OC} = \frac{\beta_a \beta_c}{2.303(\beta_a + \beta_c)R_p} \quad [2]$$

where β_a and β_c are the absolute values of anodic and cathodic Tafel constants, respectively. Tafel constants could seldom be determined reliably from the potentiodynamic scans. In calculating i_{OC}, β_a was taken to be 0.12 V/decade, assuming that one electron is transferred in the rate-controlling step of the anodic process. For copper dissolution in aerated solutions, β_c was assumed to be 0.12 V/decade when the cathodic reaction was under activation control. If the cathodic reaction was under concentration polarization, β_c was assumed infinitely large. The cathodic reaction in all the deaerated solutions was assumed to be limited by concentration polarization: $\beta_c = \infty$V/decade. The error in determining i_{OC} with estimated Tafel constants has been shown to be within the experimental scatter.[29]

Results and Discussion

Polarization studies were made in aqueous solutions of 10^{-2} M ethylenediamine with 10^{-3} M cupric sulfate, and 10^{-4} M ethylenediamine with 10^{-5} M cupric sulfate. Figures 2a and b provide the potential-pH diagrams for these solution chemistries. Table IV shows E_{OC}, R_P, and i_{OC} for each group of experiments, at each pH.

Deaerated 10^{-2} M ethylenediamine with 10^{-3} M cupric sulfate.—Figure 3 shows the effect of pH from 4.5 to 13 on the polarization behavior of the copper electrode rotating at 200 rpm in deaerated 10^{-2} M ethylenediamine with 10^{-3} M cupric sulfate aqueous solutions. The polarization behavior given in Fig. 3 is reasonably consistent with the potential-pH diagram shown in Fig. 2a. The potential-pH diagram shows that at pH 4.5, Cu_2O is stable above the copper immunity region between 206 and 296 mV. The rest potential measured at this pH was 225 mV. As the potential was scanned in the anodic direction, active dissolution was observed up to about 1500 mV, indicating that any Cu_2O or precursor phase that might have formed in this potential range was either not protective or did not form within the time scale of the experiment. The minor reduction in the current density seen above 1500 mV may suggest the formation of a hydrolyzed Cu(II) phase. In Fig. 2a, no oxide predominates at potentials exceeding 262 mV at pH 4.5. However, the increase in the local concentration of Cu(II) around the electrode after a reasonable amount of anodic dissolution may have been high

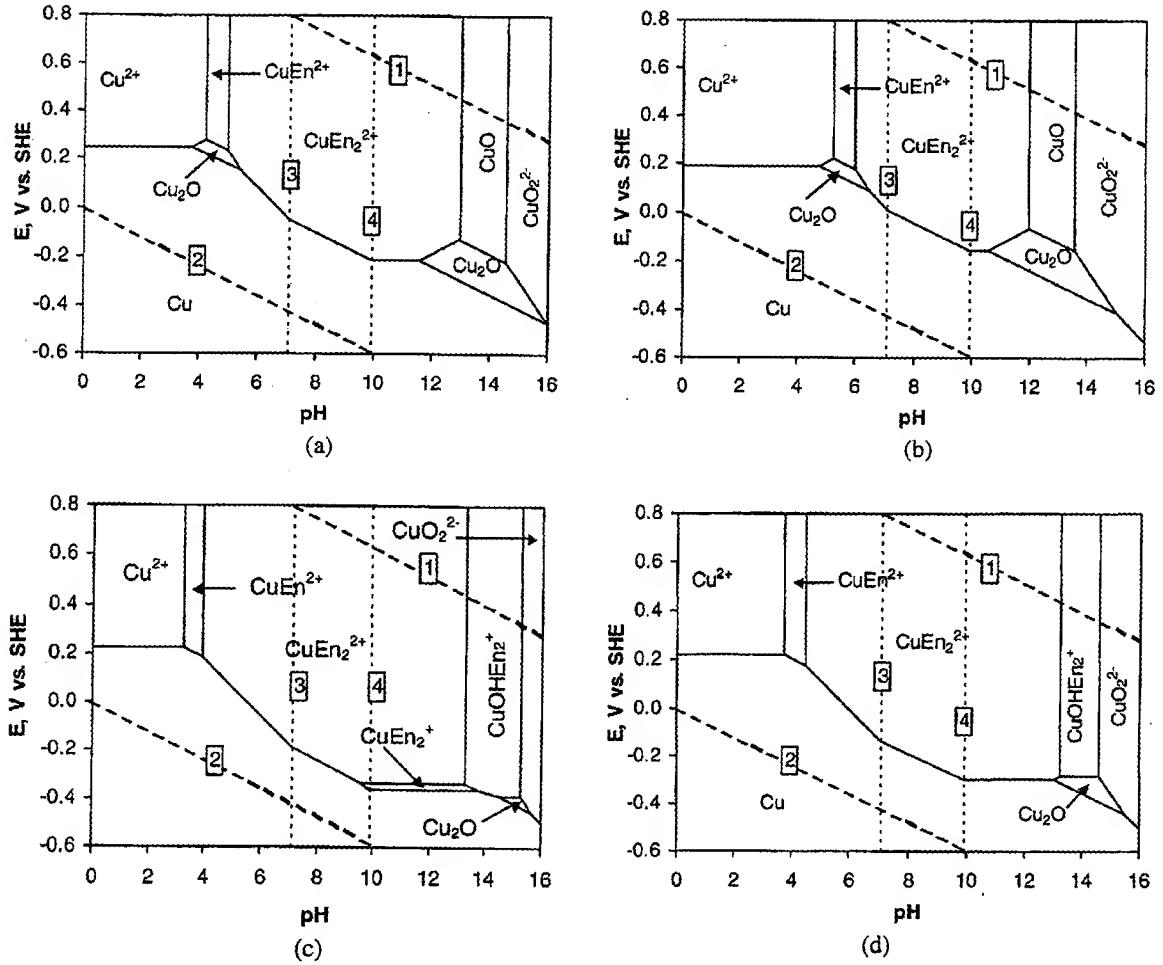

Figure 2. Potential-pH diagrams for the copper-water-ethylenediamine system at 25°C and 1 atm. (a) $\{En_T\} = 10^{-2}$ and $\{Cu_T\} = 10^{-3}$, (b) $\{En_T\} = 10^{-4}$ and $\{Cu_T\} = 10^{-5}$, (c) $\{En_T\} = 1$ and $\{Cu_T\} = 2 \times 10^{-4}$, and (d) $\{En_T\} = 10^{-1}$ and $\{Cu_T\} = 10^{-4}$.

enough to nucleate CuO, $Cu(OH)_2$, or a related phase, even when rotating at 200 rpm. Similar polarization behavior was previously observed in the copper-water-glycine system at pH values where the potential-pH diagram predicted a small stability domain of Cu_2O between the domains of copper immunity and a soluble copper glycinate phase.[4]

Figure 2a predicts that the aqueous $CuEn_2^{2+}$ species should predominate at potentials greater than the copper immunity region between about pH 5.5 and 11.5, without any formation of oxide. From about pH 11.5 to 13, Cu_2O should form first on oxidizing copper, then $CuEn_2^{2+}$ should appear at higher potentials. The polarization diagram shown in Fig. 3a indicates that at pH 9 copper actively dissolves. At this pH, the open-circuit potential was 17 mV higher than the upper limit of the copper immunity region. This suggests that the main contributor to the anodic current at E_{OC} was dissolution of Cu as $CuEn_2^{2+}$ (reaction 16 in Table III).

At pH 12, the potential-pH diagram shows that Cu_2O becomes predominant at potentials above −237 mV. The rest potential at this pH was 18 mV higher. The polarization behavior at this pH (Fig. 3b) was similar to that at pH 4.5. On polarizing anodically from E_{OC}, active dissolution was first observed, up to about 720 mV, followed by a reduction in the current densities at higher potentials. As at pH 4.5, any Cu_2O or precursor phase that may have formed in the active region was either not protective or did not form within the time scale of the experiment. Although Fig. 2a shows that no oxide would predominate at potentials above −186 mV at pH 12, the region of observed current reduction above 720 mV may suggest the formation of a hydrolyzed Cu(II) phase. The formation of such a phase could be due to local increases in the concentrations of Cu(II) and OH^- around the electrode as the potential is anodically scanned, with no local increase in the concentration of ethylenediamine.

At pH 13, the potential-pH diagram predicts the formation of Cu_2O and CuO at −296 and −127 mV, respectively. At this pH, E_{OC} dropped to −284 mV, 12 mV above the potential for equilibrium between elemental copper and Cu_2O. The anodic polarization curve shows an initial active region, followed by a minor reduction in the current density at around −80 mV, and a region between about 350 and 800 mV with significantly lowered current density. Figure 2a suggests that these reductions in current were due to the

Table IV. Open-circuit potential, polarization resistance, and current densities of copper in aqueous $CuSO_4$-ethylenediamine solutions.

Solution	pH	E_{OC} (mV, SHE)	R_P (Ωm^2)	i_{OC} (A/m^2)
10^{-2} M ethylenediamine with 10^{-3} M $CuSO_4$, deaerated	4.5	225	10.22	5.10×10^{-3}
	9	−138	6.32	8.24×10^{-3}
	12	−219	4.90	1.06×10^{-2}
	13	−284	4.22	1.23×10^{-2}
10^{-2} M ethylenediamine with 10^{-3} M $CuSO_4$, aerated	4.5	298	0.31	8.40×10^{-2}
	9	−26	0.02	1.30
	10	−78	0.03	8.68×10^{-1}
	11	−121	0.04	6.51×10^{-1}
	12	−145	0.03	1.74
	13	−168	0.02	2.61
10^{-4} M ethylenediamine with 10^{-5} M $CuSO_4$, deaerated	5.5	159	9.94	5.24×10^{-3}
	9	−72	7.92	6.58×10^{-3}
	12	−213	0.53	9.83×10^{-2}
10^{-4} M ethylenediamine with 10^{-5}M $CuSO_4$, aerated	5.5	196	0.33	7.89×10^{-2}
	9	54	0.10	2.61×10^{-1}
	10	18	0.15	1.74×10^{-1}
	11	−24	0.09	2.89×10^{-1}
	12	−74	0.06	8.68×10^{-1}

presence of cuprous and cupric oxides on the electrode surface, respectively. Cu_2O probably nucleated in the initial active region, then spread and thickened as the potential increased. From the first region of reduced current, this transformation appears to have been completed at around −80 mV. It is not unusual for the experimentally measured potentials for the onset of the reduced current region to be more noble than the equilibrium potentials for oxide formation[30-33] due to film formation kinetics,[33] including nucleation and growth.[32] Here uncompensated ohmic drops could also have contributed to the overpotential. Figure 3b shows that at pH 13, the current density increased with increasing potential above −40 mV to the onset of the second current reduction peak at around 350 mV. CuO is stable at the potentials of this active region. The increase in the current density with increasing potential suggests that when any surface Cu_2O and underlying copper are oxidized to CuO the initial product is not protective. The 430 mV displacement of the potential from the equilibrium potential for oxidation of Cu_2O to CuO probably reflects the formation of a film by a dissolution-precipitation mechanism.[34] There may also be an increased contribution from ohmic potential drops, due to the high current densities.

The copper electrode surface was bright and shiny after the polarization tests at pH 13, with no evidence of pitting. This suggests that the transpassive region exhibited at this pH corresponds to the evolution of oxygen from water

$$2H_2O = O_2 + 4H^+ + 4e \qquad [3]$$

Since it is difficult to remove oxygen completely, even after purging with nitrogen, the polarization behavior at potentials immediately below E_{OC} reflects the mass-transport controlled reduction of traces of dissolved oxygen as well as the reduction of $CuEn_2^+$ to

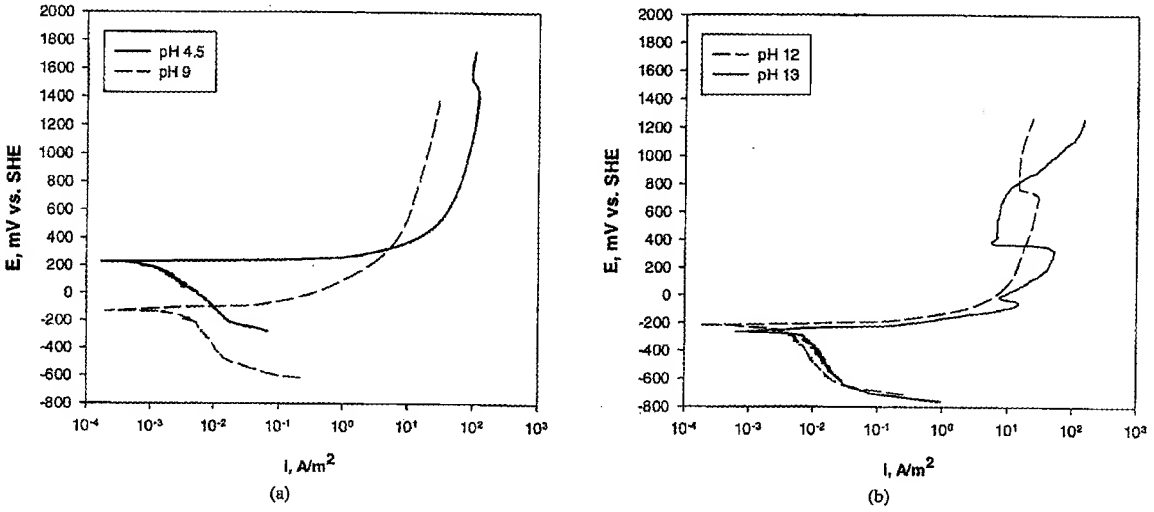

Figure 3. Effect of pH on the polarization behavior of copper in deaerated 10^{-2} M ethylenediamine, 10^{-3} M cupric sulfate at 1 mV/s and 200 rpm. (a) pH 4.5, 9; (b) pH 12, 13.

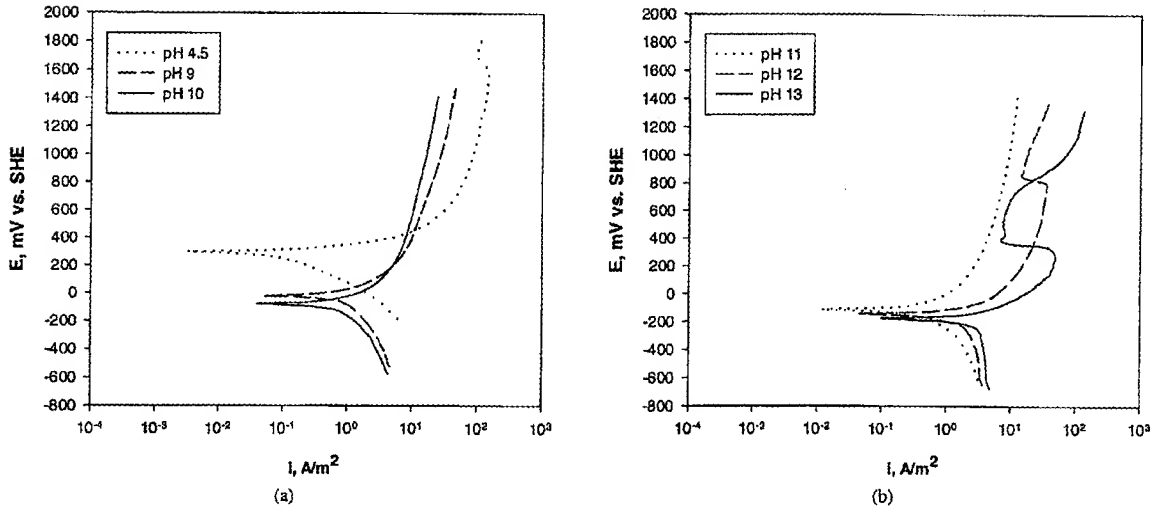

Figure 4. Effect of pH on the polarization behavior of copper in aerated 10^{-2} M ethylenediamine, 10^{-3} M cupric sulfate at 1 mV/s and 200 rpm. (a) pH 4.5, 9, 10; (b) pH 11, 12, 13.

elemental copper, or at the higher pH values, to Cu_2O. At large cathodic overpotentials there is a dramatic increase in the cathodic current density, due to the evolution of hydrogen

$$2H_2O + 2e = H_2 + 2\ OH^- \quad [4]$$

Aerated 10^{-2} M ethylenediamine with 10^{-3} M cupric sulfate.—Figure 4 shows the effect of pH from 4.5 to 13 on the polarization behavior of copper in aerated 10^{-2} M ethylenediamine, 10^{-3} M cupric sulfate aqueous solutions. As expected, the E_{OC} and i_{OC} values shown in Table IV are significantly higher than those for the deaerated system at the same pH and composition. These increases in E_{OC} and i_{OC} become more pronounced at higher pH values. Over most of the potentials scanned, the cathodic current densities were about two orders of magnitude higher than those observed under deaerated conditions at the same overpotentials in Fig. 3. The higher potentials and currents reflect cathodic reduction of oxygen

$$O_2 + 2H_2O + 4e = 4\ OH^- \quad [5]$$

The open-circuit potentials are clearly mixed potentials, with modest anodic dissolution of copper electrode at steady state. Active corrosion of copper by oxygen in aqueous ethylenediamine solutions has been reported earlier.[12]

The anodic polarization behavior for copper at pH 4.5, 9, and 12 is qualitatively similar under deaerated and aerated conditions (Fig. 3 and 4). The behavior exhibited at pH 13 is also similar, except that the minor region of reduced currents seen at about −50 mV in Fig. 3b is masked under aerated conditions (Fig. 4b), because of the higher open-circuit potential, E_{OC}. The polarization behavior of copper was also examined at pH 10 and 11 in aerated solutions. The active dissolution behavior at pH 9, 10, and 11 in Fig. 4 is consistent with the predominance of the soluble $CuEn_2^{2+}$ species at these pH values seen in Figure 2a. Table IV indicates that i_{OC} decreased on increasing the pH from 9 to 11. This could be due to the decreasing fraction of HEn^+ with increasing pH (see Fig. 1); HEn^+ has been reported to be more reactive than En.[12] Despite the decreasing fraction of HEn^+, there was an almost threefold increase in i_{OC} on increasing the pH from 11 to 12. As the pH was further increased from 12 to 13, i_{OC} almost doubled. Table IV shows that i_{OC} at pH 13 was also higher than that at pH 12 in deaerated solutions. Figure 4b shows that between −100 mV and the onset of the region of the reduced currents, anodic current densities at pH 12 were about half an order of magnitude higher than those in the same potential range at pH 11. Similarly, between −150 mV and the onset for the region of the reduced currents, the anodic current densities at pH 13 were about three times larger than those in the same potential range at pH 12. These results indicate that no protective phases or species formed at highly alkaline pH values during polarization. Indeed, any modification of the electrode surface due to aeration would appear to promote dissolution rather than suppress it.

Deaerated 10^{-4} M ethylenediamine with 10^{-5} M cupric sulfate.—Comparison of Fig. 2a and b shows that the equilibrium predominance regions of Cu_2O and CuO in the alkaline region shift to lower pH values as the solution is diluted by a factor of 100. At $\{En_T\} = 10^{-4}$ and $\{Cu_T\} = 10^{-5}$, Cu_2O is expected to form at around pH 10.5, and CuO at about pH 12. Figure 5 shows the effect of pH from 5.5 to 12 on the polarization behavior of a copper electrode rotating at 200 rpm in deaerated 10^{-4} M ethylenediamine, 10^{-5} M cupric sulfate aqueous solutions. The E_{OC} and i_{OC} values from these polarization experiments are also shown in Table IV.

The polarization curves given in Fig. 5 are fairly consistent with those in Fig. 2b, which predicts that $CuEn_2^{2+}$ would form when copper is oxidized at pH 9. On polarizing anodically from E_{OC}, copper dissolved actively at pH 9. At pH 5.5, the potential-pH diagram predicts the formation of Cu_2O above the copper immunity region at 147 mV. The rest potential measured at this pH was 12 mV higher. As the potential was scanned in the anodic direction, a large region of active dissolution was observed up to about 1400 mV, indicating that any Cu_2O or precursor phase that might have formed in this potential range was either nonprotective or was kinetically inhibited from forming. The very minor decrease in the current densities above 1400 mV may suggest the formation of a hydrolyzed Cu(II) phase. Although Fig. 2b shows no oxide predominating at potentials above 203 mV at pH 5.5, a film of some Cu(II) phase may have developed due to local modification of the solution chemistry around the electrode after a reasonable amount of anodic dissolution, even when rotating at 200 rpm.

At pH 12, Fig. 2b predicts the formation of Cu_2O and CuO at −237 and −68 mV, respectively. At this pH, E_{OC} dropped to −213 mV, 24 mV above the potential for equilibrium between el-

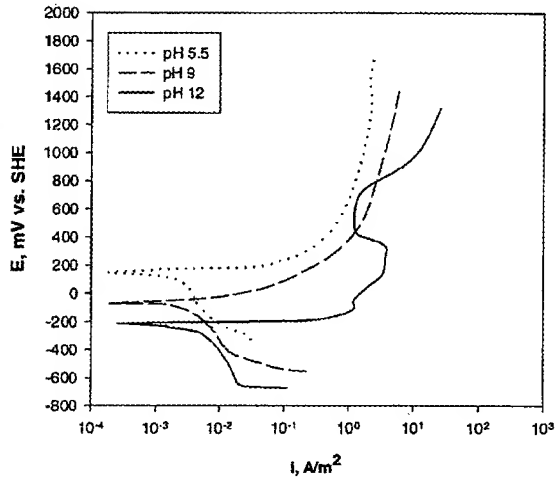

Figure 5. Effect of pH on the polarization behavior of copper in deaerated 10^{-4} M ethylenediamine, 10^{-5} M cupric sulfate at 1 mV/s and 200 rpm.

emental copper and Cu_2O. The anodic polarization curve shows an initial active region, followed by a minor reduction in the current density at around −100 mV, and a region between about 300 and 700 mV with significantly lowered current density. Figure 2b suggests that these reductions in current were due to the presence of cuprous and cupric oxides on the electrode surface, respectively. Cu_2O probably nucleated in the initial active region, then spread and thickened as the potential increased up to −100 mV. The increase in the current density with increasing potential indicates that the Cu(II) solid phase initially developing between −50 mV to the onset of the second current reduction peak at 350 mV is not protective. The displacements of the potential for oxidation of Cu to Cu_2O and Cu_2O to CuO probably reflect the slow kinetics associated with film formation, although uncompensated ohmic drops may also contribute.

Aerated 10^{-4} M ethylenediamine with 10^{-5} M cupric sulfate.—Figure 6 shows the effect of pH from 5.5 to 12 on the polarization behavior of copper in aerated 10^{-4} M ethylenediamine, 10^{-5} M cupric sulfate aqueous solutions. E_{OC} and i_{OC} values at each pH are also tabulated in Table IV. As expected, these are significantly higher than those for the deaerated system at the same pH and composition due to the availability of oxygen for reduction.

The anodic polarization behavior for copper at pH 5.5 and 9 is very similar in Fig. 5 and 6. The behavior exhibited at pH 12 is also similar, except that the minor region of reduced current seen at about −100 mV in deaerated conditions is masked under aerated conditions. The polarization behavior of copper was also examined at pH 10 and 11 in aerated solutions. The active dissolution behavior at pH 9 and 10 in Fig. 6 is consistent with that of Fig. 2b. Table IV indicates that i_{OC} decreased somewhat on increasing the pH from 9 to 10, probably due to the decreasing fraction of HEn^+. At pH 11, the potential-pH diagram predicts the predominance of Cu_2O above the copper immunity region at −178 mV, and below the $CuEn_2^{2+}$ predominance region at −128 mV. As the potential was scanned in the positive direction from E_{OC}, a large region of active dissolution was observed up to about 900 mV, indicating that any Cu_2O or precursor phase that may have formed in this potential range was either not protective or was kinetically unable to form. Above 900 mV some reduction in the current density was noticeable, probably due to the formation of a film of some hydrolyzed Cu(II) phase formed in response to local changes in the solution chemistry near the electrode after a reasonable amount of anodic dissolution. Despite the decreasing fraction of HEn^+, i_{OC} increased on increasing the pH from 10 to 12, suggesting that any modification of the electrode surface due to aeration promoted dissolution. The copper electrode surface was bright and shiny after the polarization tests at pH 12, with no evidence of pitting. This may suggest that the transpassive region exhibited at this pH corresponds to the evolution of oxygen from water.

Conclusions

The electrochemistry of copper in aqueous ethylenediamine solutions was investigated by comparing the polarization behavior with appropriate potential-pH diagrams. Due to its complexation action, ethylenediamine increased the solubility range of copper to

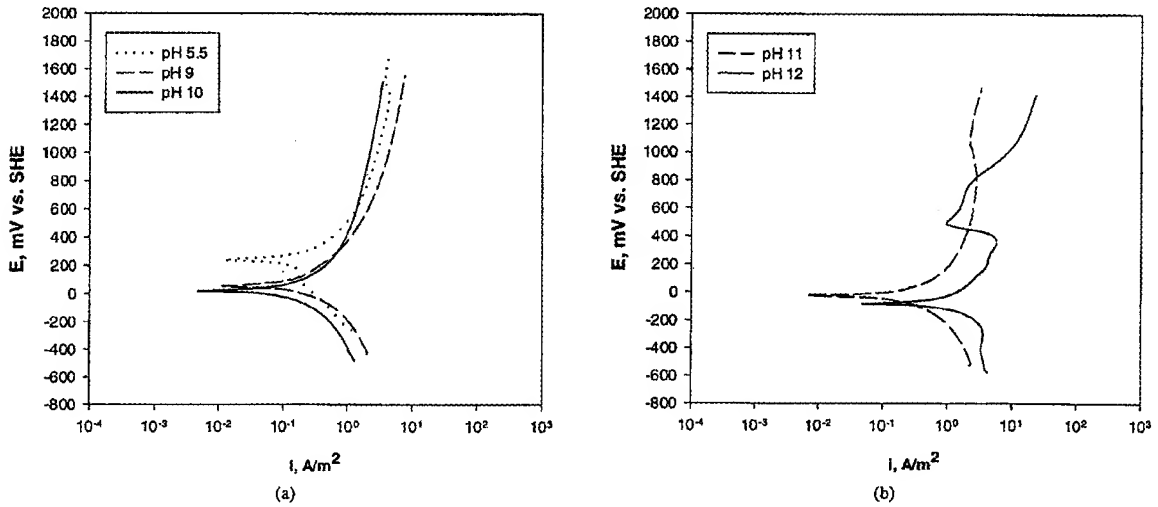

Figure 6. Effect of pH on the polarization behavior of copper in aerated 10^{-4} M ethylenediamine, 10^{-5} M cupric sulfate at 1 mV/s and 200 rpm. (a) pH 5.5, 9, 10; (b) pH 11, 12.

lower potentials and higher pH values. The stability regions of CuO and Cu_2O contracted with increasing amounts of ethylenediamine. The polarization behavior agreed well with the thermodynamic potential-pH diagrams. The anodic dissolution rate of copper in ethylenediamine solutions was controlled by the solution pH, concentrations of dissolved oxygen, and ethylenediamine.

The University of California at Berkeley assisted in meeting the publication costs of this article.

References

1. M. Pourbaix, *Atlas of Electrochemical Equilibria in Aqueous Solutions*, p. 384, Pergamon Press, London (1965).
2. M. Pourbaix, *Lectures on Electrochemical Corrosion*, p. 49, Plenum, New York (1973).
3. H. E. Johnson and J. Leja, *J. Electrochem. Soc.*, **112**, 638 (1965).
4. S. Aksu and F. M. Doyle, *J. Electrochem. Soc.*, **148**, B51 (2001).
5. S. I. Berezina, Y. G. Voitsekhokii, A. V. Ilyasov, and B. G. Yavisev, *Prikl. Electrokhim.*, 1-2, 62 (1973).
6. S. M. Beloglazov and A. S. Milushkin, *Korroz. Zashch. Mat.*, **3**, 126 (1977).
7. S. Mizumoto, H. Nawafune, T. Hiroo, Y. S. Zhang, and M. Haga, *Hyomen Gijutsu*, **43**, 978, (1992).
8. S. Jayakrushnan, R. M. Krishnan, S. Sriveeraraghavan, N. Kaplana, and T. Umashankar, *Trans. Met. Finish. Assoc. India*, **6**, 275 (1997).
9. W. K. Choi and W. Z. Oh, *J. Nucl. Sci. Technol.*, **30**, 549 (1993).
10. R. Latha, S. Rangarajan, S. V. Narasimhan, S. Rajeswari, and M. Subbaiyan, in *Proceedings of the International Conference on Corrosion* CONCORN, Mumbai, India, p. 1224 (Dec 1997).
11. A. Vaškelis, E. Norkus, J. Reklaitis, and J. Jačiauskienė, *Chemija*, **3**, 199 (1998).
12. J. Halpern, H. Milant, and D. R. Wiles, *J. Electrochem. Soc.*, **106**, 647 (1959).
13. J. Halpern, *J. Electrochem. Soc.*, **100**, 421 (1953).
14. S. C. Sircar and D. R. Wiles, *J. Electrochem. Soc.*, **107**, 164 (1960).
15. L. H. Jenkins, *J. Electrochem. Soc.*, **107**, 371 (1960).
16. A. El-Sayed, F. Rahwan, and F. El-Cheikh, *Mater. Chem. Phys.*, **46**, 61 (1996).
17. A. Survila and A. Surviliene, *Chemija*, **10**, 188 (1999).
18. A. Survila, A. Surviliene, and G. Stalnionis, *Chemija*, **10**, 203 (1999).
19. R. M. Smith and A. E. Martell, *Critical Solubility Constants*, Vol. 1, 5, and 6, Plenum, New York (1977).
20. L. G. Sillen and A. E. Martell, *Stability Constants of Metal-Ion Complexes*, Special Publications N17 and 25, Chemical Society, London, Vol. 1 (1964), Vol. 2 (1971).
21. D. D. Wagman, W. H. Evans, V. B. Parker, R. H. Schumm, I. Halow, S. M. Bailey, K. L. Churney, and R. L. Nuttall, *J. Phys. Chem. Ref. Data Suppl.*, **11**, Supplement No. 2 (1982).
22. J. Van Muylder, in *Comprehensive Treatise of Electrochemistry*, J. O'M. Bockris, B. E. Conway, E. Yeager, and R. E. White, Editors, Vol. 4, p. 1, Plenum Press, New York (1981).
23. D. Tromans and J. C. Silva, *Corros. Sci.*, **53**, 16 (1997).
24. D. Tromans, *J. Electrochem. Soc.*, **145**, L42 (1998).
25. A. J. Bard and L. R. Faulkner, *Electrochemical Methods*, p. 71, John Wiley & Sons, Inc., New York (1980).
26. *Handbook of Chemistry and Physics*, 81st ed., D. R. Lide, Editor, p. 5-94, CRC Press, Boca Raton FL (2001).
27. M. Stern and A. L. Geary, *J. Electrochem. Soc.*, **104**, 56 (1957).
28. M. Stern and M. Weisert, *Proc. ASTM.*, **59**, 1280 (1959).
29. Denny A. Jones, *Principles and Prevention of Corrosion*, p. 146, Prentice-Hall, Upper Saddle River, NJ (1996).
30. H. H. Strehblow and B. Titze, *Electrochim. Acta*, **25**, 839 (1980).
31. S. L. Marchiano, C. I. Elsner, and A. J. Arvia, *J. Appl. Electrochem.*, **10**, 365 (1980).
32. M. R. Gennero De Chialvo, S. L. Marchiano, and A. J. Arvia, *J. Appl. Electrochem.*, **14**, 165 (1984).
33. W. Kautek and J. G. Gordon II, *J. Electrochem. Soc.*, **137**, 2672 (1990).
34. N. D. Tamashov and G. P. Chernova, *Passivity and Protection of Metals Against Corrosion*, p. 38, Plenum Press, New York (1967).